Green Chemistry

CRITICAL REVIEW

Cite this: *Green Chem.*, 2015, **17**, 2647

CO_2 methanation over heterogeneous catalysts: recent progress and future prospects

M. A. A. Aziz,[a] A. A. Jalil,[a,b] S. Triwahyono*[c] and A. Ahmad[a,b]

Received 19th January 2015,
Accepted 6th March 2015

DOI: 10.1039/c5gc00119f

www.rsc.org/greenchem

Catalytic approaches for CO_2 fixation can play an important role, because CO_2 can be artificially converted into reusable chemicals. Among the catalytic reactions of CO_2, hydrogenation of CO_2, the so-called methanation reaction, is a suitable technique for the fixation of CO_2. This technique can be used to convert exhausted CO_2 into methane (CH_4), which can be recycled for use as a fuel or a chemical as well as by contributing to the reduction of CO_2 emissions. Heterogeneous catalysts have been used to hydrogenate CO_2 to methane. Heterogeneous catalysts are preferable to homogenous catalysts in terms of stability, separation, handling, and reuse, which reflects in lower costs for large-scale production. Significant progress has been made in this direction, the exploitation of novel heterogeneous catalysts. In this review, we discussed recent developments in this area, with emphases on catalytic reactivity and its physicochemical properties and reaction mechanism. Apart from materials aspects and catalytic performance, we also discuss fundamental strategies for the rational design of materials for effective transformation of CO_2 to methane with the help of H_2 and power sources.

Introduction

Global warming-induced climate change is one of the significant threats to civilization of modern times.[1] Increases of greenhouse gases (GHGs) in the atmosphere produce a positive radiative forcing of the climate system and a consequent warming of surface temperatures and rising sea level caused by thermal expansion of the warmer seawater. In addition, it also contributes to melting in glaciers and ice sheets as well as to the environmental factors such as agriculture, water resources, and human health.[2] Although other factors exist, the importance of the aforementioned relationship should not be overlooked. Unfortunately, it is predicted that this trend of increasing atmospheric GHG concentration will not be altered within the next several decades, because fossil fuels will be still the dominant energy source.

CO_2 has covered about 82% of total GHGs. Therefore, CO_2 as a raw material has been a focus in the CO_2-reduction research area. This is due to the advantages of CO_2 which is attractive as highly functional, widely available, inexpensive, renewable carbon source and an environmentally friendly chemical reagent.[3,4] The different proposed technologies follow one of two major approaches: to capture and geologically sequester CO_2, or to convert CO_2 into useful low-carbon fuels. In today's world of high energy demands, CO_2 conversion and utilization seems to be a more attractive and promising solution. Presently, the use of CO_2 as chemical feedstock is limited to a few industrial processes; synthesis of urea and its derivatives, salicylic acid, carbonates and methanol.[5–8] This increasing interest is focused on the concept of recovered CO_2 being used to synthesize fuels (through, for example, Fischer–Tropsch chemistry), and such an approach could reduce substantially carbon emissions.[9] The products of CO_2 hydrogenation such as methanol and dimethyl ether (DME) are excellent fuels in internal combustion engines, and also are easy for storage and transportation. Although the production of methanol and DME from CO_2 are promising processes these need to be performed under reaction high pressures (~5 Mpa).[10] In addition, the literature showed that the CO_2 conversion to methanol is still very low (<20%) and it is difficult to achieve 100% conversion of CO_2.[11] The CO_2 hydrogenation to methane (CO_2 methanation) presents several advantages over other chemicals because it can be injected directly into already existing natural gas pipelines, and it can be used as a fuel or raw material for the production of chemicals. In addition, methane formation from CO_2 is a more simple reaction which can generate methane under atmospheric pressure. Furthermore, the formation of CH_4 from CO_2 at (low) room temperature has become an important breakthrough in the knowledge of the role and in the use of CO_2, although the conversion was still very low.[12]

[a]*Institute of Hydrogen Economy, Universiti Teknologi Malaysia, 81310 UTM Johor Bahru, Johor, Malaysia*
[b]*Department of Chemical Engineering, Faculty of Chemical Engineering, Universiti Teknologi Malaysia, 81310 UTM Johor Bahru, Johor, Malaysia*
[c]*Department of Chemistry, Faculty of Science, Universiti Teknologi Malaysia, 81310 UTM Johor Bahru, Johor, Malaysia. E-mail: sugeng@utm.my*

CO_2 methanation remains the most advantageous reaction with respect to thermodynamics, since the reaction is considerably faster than other reactions which form hydrocarbons or alcohols.[13] This CO_2 methanation reaction is called the Sabatier reaction and could be applied in industry, provided that hydrogen is generated from renewable sources.

$$CO_2 + 4H_2 \leftrightarrow CH_4 + 2H_2O \qquad \Delta G_{298} = -114 \text{ kJ mol}^{-1} \quad (1)$$

The methanation of carbon dioxide is an important catalytic process of fundamental academic interest with potential commercial application.[14–16] Because the interest in the large-scale manufacture of substitute natural gas from the products of coal gasification has greatly diminished in recent decades,[17] carbon dioxide methanation, in the fuel cell and ammonia synthesis industry, can be used for the removal of trace CO from H_2-rich streams to prevent catalyst poisoning.[18] In addition, the National Aeronautics Space Administration (NASA) is also interested in applications of the Sabatier reaction for use in future manned space colonization on Mars.[15] Bringing Terrene hydrogen to Mars will make it possible to convert the Martian carbon dioxide atmosphere into methane and water for fuel and astronaut life-support systems.[19]

In recent years, CO_2 methanation *via* heterogeneous catalysts has recently attracted a considerable amount of attention, as demonstrated by the burgeoning number of publications (Fig. 1). Metals, such as Ru, Rh, Ni, Co, and so forth on various supports have been reported to be effective methanation catalysts. The latest review on CO_2 methanation on various catalytic system was conducted by Wang *et al.*[20] However, the review primarily focused on general aspects of CO_2 methanation, was published 3 years ago and no later report has been published yet. Therefore, the present review attempts to provide current understanding of the catalytic performance and insight into the reaction mechanism over heterogeneous catalysts between January 2011 and January 2015, as well as the future prospects of CO_2 methanation.

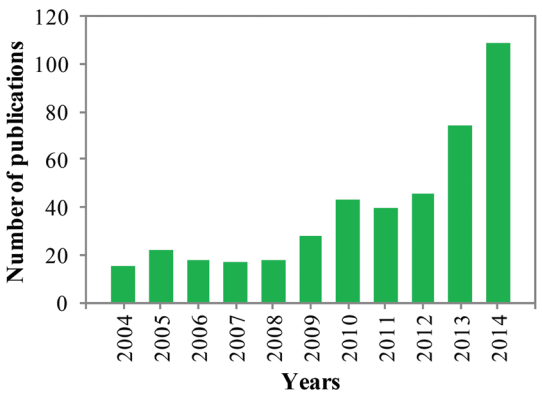

Fig. 1 Number of publication dealing with CO_2 methanation *versus* years (2004–2014) extracted from ISI Web of Science (Thomson Reuters) database retrieved using the keywords "CO_2 methanation".

Metal-based heterogeneous catalysts

Ni-based catalysts

Hydrogenation of CO_2 toward methane has been extensively studied using supported nickel catalysts.[21–58] Ni-based catalysts have been widely investigated for industrial purposes due to their low cost and easily availability. The methanation of carbon dioxide over Ni catalysts was studied in detail by a lot of researchers at the laboratory scale because of the theoretical significance and possible practical application of this reaction. The performance of catalysts toward CO_2 methanation is dependent on various parameters such as the effect of support, the effect of nickel loading, the effect of a second metal and the effect of the preparation method.

Effect of support. Because the support has a significant influence on the morphology of the active phase, adsorption, and catalytic properties,[59] preparation of highly dispersed supported metal catalysts has been the focus of significant research. Therefore, high surface area supports, usually oxides, are used extensively in industry for the preparation of metal catalysts including silica, alumina, silica–alumina, and zeolites. Tada *et al.* has studied the effect of various supports (CeO_2, α-Al_2O_3, TiO_2 and MgO) on Ni catalysts for CO_2 methanation.[26] From their report, Ni/CeO_2 showed high CO_2 conversion, especially at low temperatures, compared to Ni/α-Al_2O_3, and the selectivity to CH_4 was very close to 100%. As shown in Fig. 2, Ni/CeO_2 shows the highest yield to methane followed by Ni/α-Al_2O_3, Ni/TiO_2 and Ni/MgO. The surface coverage by CO_2-derived species on the CeO_2 surface and the partial reduction of CeO_2 surface could result in high CO_2 conversion over Ni/CeO_2.[26] The excellent CeO_2 support led to the study of different support materials for methanation of CO_2, including SiO_2, Al_2O_3, ZrO_2, and CeO_2, doped with a different percentage of active nickel and cobalt metals using a standard

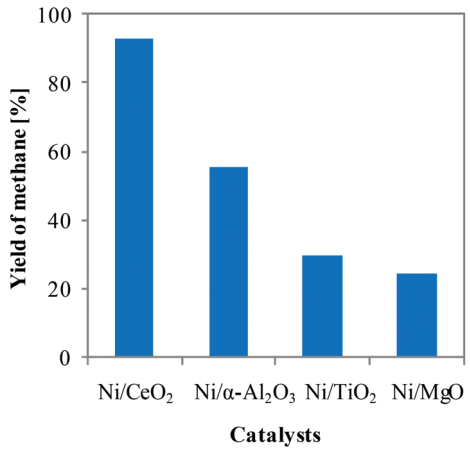

Fig. 2 Effect of support materials on yield of methane over Ni/CeO_2, Ni/a-Al_2O_3, Ni/TiO_2, and Ni/MgO. Reaction conditions: reaction temperature = 350 °C, 20 vol.% CO_2, 80 vol.% H_2, GHSV = 10 000 h^{-1}. Results are calculated based on the conversion of CO_2 and selectivity to CH_4 adopted from Tada *et al.*[26]

coprecipitation method.[28] It was found that the ZrO_2–CeO_2-supported catalyst can attain ≥95% CO_2 conversion at 400 °C and has a CH_4 selectivity of 99%.[28]

The hydrogenation of carbon dioxide, producing methane and CO, has been investigated over Ni/Al_2O_3 catalysts.[52] Catalytic activity needs the presence of Ni metal particles which may form *in situ* if the Ni loading is higher than that needed to cover the alumina surface with a complete monolayer. If the Ni content is lower, pre-reduction is needed. Catalysts containing very small Ni particles obtained by reducing moderate loading materials are very selective to methane without CO formation. The larger the Ni particles, due to higher Ni loadings, the higher the CO production. Cubic Ni metal particles are found in the spent catalysts mostly without carbon whiskers. The fast methanation occurs at the expense of CO intermediate on the corners of nanoparticles interacting with alumina, likely with a "*via* oxygenate" mechanism.[52] Abello *et al.* has reported the methanation of carbon dioxide over a high-loaded Ni–Al mixed oxide catalyst (*ca.* molar ratio Ni/Al = 5).[51] Despite the high nickel loading (*ca.* 70 wt%), which is theoretically thought to be counterproductive for the nickel-based catalyst performance, the Ni–Al activated catalyst exhibited high CO_2 conversion, and rendered a CH_4 selectivity very close to 100%. This is originated by the formation of small metallic nickel crystallites (*ca.* 6 nm) dispersed over NiO–alumina upon partial reduction of the mixed oxide. The catalyst experiences complete reduction during reaction, which increases slightly the Ni crystallite size, but preserves the high activity in *ca.* 500 h lifetime tests even at high space velocity.[51]

Recently, the important of support was clearly observed when nickel nanoparticles (NPs, particle radius <8 nm) were compared to 125% Ni/Al_2O_3 tested on CO_2 methanation.[53] At 773 K, the best catalytic activity was obtained on 125% Ni/Al_2O_3, while Ni NPs resulted as poorly active in catalysing this reaction. The support effect is evident in the methanation of CO_2 on Ni/Al_2O_3, thought to justify the high activity of this catalyst and the very low activity of Ni NP in this reaction.[53]

Zeolite and TiO_2 are among the supports used for Ni catalysts in CO_2 methanation. High catalytic activity of sorption catalysts based on Ni/zeolite was due to the properties of zeolites, which are chemically active nanostructures and have space for enhancing the sorption properties of the catalysts.[37] Therefore, CO_2 hydrogenation into methane was carried out over catalysts containing nickel and cerium species supported on a HNaUSY zeolite.[48] An enhancement of the catalysts' performances was noticed when doping the Ni–zeolites catalysts with 3–15% Ce. The presence of CeO_2 after reduction might promote CO_2 activation into CO. Comparing these results with those reported in the literature, it is possible to conclude that zeolites have great potential to be used as catalyst supports for the CO_2 methanation reaction.[48] Ni nanoparticles (NPs) on a TiO_2 support were synthesized *via* a deposition–precipitation method followed by a calcination–reduction process. The Ni NPs are highly dispersed on the TiO_2 surface (particle size: 2.2 nm), with a low Ni–Ni coordination number.[35]

Recently, ceria–zirconia mixed oxides have become one of the potential supports for the CO_2 methanation reaction. They turned out to be greatly efficient in terms of activity and stability due to their high oxygen storage capacity and properties to activate CO_2.[23,33] In addition, the interactions between Ni and the ceria–zirconia support were found to be a key parameter for the methanation reaction.[33] Ocampo *et al.* first reported carbon dioxide methanation over a series of Ni–$Ce_xZr_{1-x}O_2$ catalysts prepared by a pseudo sol–gel method.[23] The catalysts gave impressive CO_2 conversion and extremely high selectivity to methane (superior to 98%). The incorporation of Ni^{2+} into the ceria–zirconia structure was proved to enhance the catalysts' specific activity. Their high activity was dependent on the surface of available metallic nickel, the composition of the support (CeO_2/ZrO_2 = 60/40) and on its modification by Ni^{2+} doping.[23] This indicated that the nature of the support plays a crucial role in the interaction between the nickel and the support, and thus determines catalytic performance toward activity and selectivity for the methanation of CO_2.

In contrast to Ocampo *et al.* which reported a composite catalysts support for CeO_2/ZrO_2 catalysts, Liu *et al.* tested the performance of a CeO_2/Al_2O_3 support catalyst with 15 wt% of nickel content prepared *via* impregnating boehmite.[34] The catalyst was found to be highly active and stable for methanation of carbon dioxide with hydrogen at a H_2/CO_2 molar ratio of 4. The catalytic performance was strongly dependent on the CeO_2 content in Ni–CeO_2/Al_2O_3 catalysts and the catalysts with 2 wt% CeO_2 had the highest catalytic activity among those tested at 350 °C. The addition of CeO_2 decreased the reduction temperature by altering the interaction between Ni and Al_2O_3, and improved the reducibility of the catalyst. Preliminary stability tests of 120 h on-stream over the Ni–2CeO_2/Al_2O_3 catalyst at 350 °C revealed that the catalyst was much better than the unpromoted one (without CeO_2).[34]

Novel nickel-based catalysts with a nickel content of 12 wt% were prepared with the zirconia–alumina composite as support.[21] ZrO_2 was reported to improve the alumina support for CO_2 methanation. The new Ni catalyst with a new support (ZrO_2–Al_2O_3) showed higher catalytic activity and better stability than Ni/γ-Al_2O_3. The highly dispersed zirconium oxide on the surface of γ-Al_2O_3 inhibited the formation of a nickel aluminate-like phase, which was responsible for the better dispersion of Ni species and easier reduction of NiO species, leading to the enhanced catalytic performance of the catalyst.[21] The effect of ZrO_2 was also studied on the Ni/SiO_2 system for CO_2 methanation.[25] However, the effect of ZrO_2 on Ni/SiO_2 is less relevant for the methanation of CO_2. From their report, the addition of ZrO_2 is significant only on the methanation of CO due to the active surface of ZrO_2 which is able to adsorb CO.[25] The role of Ni was reported as a dissociation site for hydrogen and less capable to adsorb CO_2.[27] In the methanation of CO_2 over the mixing of Rh/γ-Al_2O_3 and Ni/activated carbon, methane is produced with 100% selectivity due to a significant synergy between the mixing of two different catalysts.[27]

It is widely accepted that the surface defects of nanocatalysts serving as an active site play a decisive role in the adsorption and reactivity of catalytic reactions. The formation or introduction of abundant and specific defect sites on the surface of supported nanocatalysts is a promising approach for tailoring the surface morphology and electronic structure to enhance heterogeneous catalytic activity.[60–62] Therefore, a flower-like Al_2O_3 matrix was fabricated as a surface defect and used with an Ni nanocatalyst for CO_2 methanation.[39] The Ni nanocatalyst shows high dispersion and high particle density embedded on the hierarchical Al_2O_3 matrix and exhibits excellent activity and stability for the reaction of CO_2 methanation. Abundant surface vacancy clusters served as active sites, accounting for the significantly enhanced low-temperature activity of the supported Ni nanoparticles. In addition, the anchoring effect from the support gives rise to a high reaction stability, without sintering and/or aggregation of active species during long-term use.[39]

Another excellent support with surface defects has been recently reported by Aziz *et al.*[41] They reported the potential of mesostructured silica nanoparticles (Ni/MSN) as a support for Ni catalysts for CO_2 methanation. The sequence of catalytic activity under various catalyst supports is as follows: Ni/MSN > Ni/MCM-41 > Ni/HY > Ni/SiO_2 > Ni/γ-Al_2O_3. The Ni/MSN catalyst exhibited the highest activity even at low temperatures (573 K). The high activity of Ni/MSN is due to the presence of both intra- and inter-particle porosity which led to the high concentration of basic sites and/or oxygen vacancy sites. The methanation activity increased with increasing concentration of basic sites. The presence of defect sites or oxygen vacancies in MSN was responsible for the formation of surface carbon species, while Ni sites dissociated hydrogen to form atomic hydrogen. The surface carbon species then interacted with atomic hydrogen to form methane. The Ni/MSN catalyst also performed with good stability and no deactivation for up to 200 h.[41]

Recently, metal–organic framework (MOF) materials has emerged as catalyst supports because they have very high surface areas, up to and more than 1000 $m^2\ g^{-1}$. Zhen *et al.* explored the potential of MOFs for heterogeneous CO_2 methanation.[55] In their work, Ni@MOF-5 was used as a support for catalysts of CO_2 methanation. A very high dispersion of Ni(41.8%) over MOF-5 (2961 $m^2\ g^{-1}$) has been achieved in this catalyst. These highly uniform, dispersed Ni in the framework of MOF-5 resulted in significant activity enhancement at low temperature. The catalyst showed almost no deactivation in long term stability tests up to 100 h.

Over the past several years, natural clays have attracted considerable attention due to their environmental compatibility, low cost, high selectivity, reusability and operational simplicity. Usually raw clays are not suitable for catalyst supports due to their small specific surface area. However, after proper modification, *e.g.*, by forming a pillared structure[27] or by acid treatment,[28] the surface area can be increased significantly. The reason why the removal of a fraction of aluminum in clay *via* acid treatment can lead to a much larger specific surface area is due to the formation of macro–mesopores, which can be used further to confine Ni species or fix them at specific sites to prevent them from sintering to a certain degree during the reaction.

In this light, Lu *et al.* has reported the usage of raw bentonite (RB) and acid–alkali treated bentonite (B) as support for Ni catalysts and tested them for the methanation of CO_2 to produce synthetic natural gas (SNG).[56] The results showed that the Ni catalysts supported on the B support were more active than those supported by RB because of the improved dispersion of Ni particles on the former that had a larger specific surface area due to the generation of mesopores within the catalyst. Therefore, proper treatment of the RB support is beneficial for the dispersion of Ni species, which is important for the high activity of CO_2 methanation.

The clay was also modified with a mesoporous-zirconia supported Ni catalyst as reported by Lu *et al.*[57] It is found that the zirconia-modified clays have a typical bimodal pore size distribution. Most of the pores with sizes smaller than 10 nm result from zirconia pillared clays and the mesopores with sizes larger than 10 nm and macropores with sizes larger than 50 nm result from the partly damaged clay layers. The bimodal pore structure is beneficial for the dispersion of Ni on the layers of the zirconia-modified clays and the zirconia nanoparticles are highly dispersed on the partly damaged clay layers.

Different types of support possessed different orders of basicity. In general, the generation of basic sites on the surface oxide of the catalyst can be exposed by pretreatment at high temperature.[63] The nature of the basic sites generated by removing the molecules covering the surfaces depends on the severity of the pretreatment. Mori and co-workers investigated the effect of various supports for Ni catalysts and found the reactivity of the catalysts depended strongly on the kind of support in the order γ-$A1_2O_3$ ≈ MgO ≈ SiO_2 > α-$A1_2O_3$ > TiO_2 ≈ SiO_2–$A1_2O_3$.[64] The reason for the higher activity of the Ni/MgO catalyst was attributed to the basic properties of the MgO support on which CO_2 could be strongly adsorbed and kept on the catalyst even at higher temperatures. Incorporation of suitable promoters is believed to improve the basicity, metal dispersion and reducibility of the catalyst. It is believed that the rare earth oxide will impart adequate basicity to the methanation catalysts, thus improving the activity. Among the rare earth oxides, CeO_2 and La_2O_3 are commonly used as promoters for hydrogenation.[65] The higher basicity of the catalyst promoted the lowering of the reaction temperature. For instance, the amount of CO_2 adsorbed on Ni/CeO_2 demonstrated by CO_2-TPD was much larger than that on Ni/α-Al_2O_3. From these results, CO_2 reduction to CO over Ni/CeO_2 can be enhanced at low temperatures compared to Ni/α-Al_2O_3. Therefore, Ni/CeO_2 displayed excellent activity for CO_2 methanation resulting in prompt conversion of CO, and consequently in high CH_4 selectivity.[26] A similar result was observed by Xavier *et al.* in which the CeO_2 doped on Ni/Al_2O_3 improved the reducibility and thus lowered the reaction temperature.[66] Ni/Ceria–zirconia mixed oxide and Ni–silica were compared in CO_2 methanation because of their properties to activate CO_2.[33]

The better activity of Ni/ceria–zirconia compared to Ni–silica can be explained by the importance of weak basic sites the adsorption of CO_2.

In summary, the nature of the support plays a crucial role in high activity of CO_2 methanation. Single metal oxides, mixed oxides, zeolites, mesoporous materials and clay possessed different characteristic and showed good potential to be used as supports for Ni catalysts. For example, CeO_2 has shown to be an excellent support due to its high oxygen storage capacity and its properties to activate CO_2. The addition of CeO_2 onto another oxide material (*i.e.* Al_2O_3) can decrease the reduction temperature by altering the interaction between Ni and Al_2O_3, and improve the reducibility of the catalyst. Other mixed oxide support such as ZrO_2 and Al_2O_3 also exhibited high activity toward CO_2 methanation. ZrO_2 improved the alumina support for CO_2 methanation by inhibiting the formation of a nickel aluminate-like phase, which was responsible for the better dispersion of Ni species and easier reduction of NiO species. Meanwhile, the high catalytic activity of Ni/zeolite was due to its active nanostructures as well as possessing a large space for enhancing the sorption properties of the catalysts. The formation or introduction of abundant and specific defect sites on the surface of supported nanocatalysts is a promising approach to enhance CO_2 methanation. This will include a flowerlike Al_2O_3 matrix, mesostructured silica nanoparticles and metal–organic framework (MOF) materials. The presence of defect sites or oxygen vacancies in MSN and high surface area of MOFs were responsible for the high activity of the catalytic reaction. Natural clays could also be a good support after proper modification (*i.e.* by forming a pillared structure or by acid treatment) to generate a larger specific surface area with the formation of macro–mesopores. Some of the potential clays are raw bentonite, acid–alkali treated bentonite and zirconia-modified clays. The high basicity of the catalyst is of importance due to its role to promote the lowering of reaction temperature. Therefore, basicity of catalyst could be a vital factor for the high activity of CO_2 methanation.

Effect of nickel loading. Nickel loading on the support was found to be affected both the interaction of nickel with the support and the nickel dispersion on the support (Ni particle sizes), which further affected the catalytic behavior during methanation. In general, the metal species tend to be highly dispersed across the carrier at low metal loadings, whereas the metal particles tend to aggregate at high metal loadings, forming large particles. Understanding this relationship can help researchers to understand dispersion–activity relationships and prepare active, selective, and stable Ni catalysts. The effect of nickel content on the structure and activity of co-precipitated Ni–Al layered double hydroxides (LDHs) as catalyst precursors for CO_2 methanation was studied by variation of the Ni^{2+}/Al^{3+} molar ratio (Ni^{2+}/Al^{3+} = 3.0, 1.5 and 0.5).[29] After reduction at 400 and 450 °C, a sample of Ni^{2+}/Al^{3+} = 3.0 demonstrated the highest conversion degree at all the reaction temperatures and space velocities.[29] The effect of Ni NPs loading on TiO_2 shows that 15 wt% of Ni exhibits excellent catalytic behavior towards CO_2 methanation (conversion: 96%; selectivity: 99%) at reaction temperature as low as 260 °C.[35] The good dispersion of Ni NPs with large unsaturation facilitates a high exposure of active sites, which accelerates the formation of surface-dissociated hydrogen and the subsequent hydrogenation removal of surface nickel carbonyl species, accounting for the resulting enhanced low-temperature catalytic performance.[35]

The effect of Ni content on mesoporous nanocrystalline γ-Al_2O_3 with high surface area was investigated in the carbon dioxide methanation reaction.[49] As shown in Fig. 3, the catalytic results showed that the CO_2 conversion increased with increasing Ni content from 10 to 20 wt%. Increasing nickel loading higher than 20 wt% decreased the yield of methane, due to a decrease of the nickel dispersion as a result of bigger crystallite size. The increasing in nickel content from 10 to 25 wt% increased the reducibility of catalyst. The catalytic results revealed that the catalyst with 20 wt% Ni possessed high activity and stability in CO_2 methanation reaction.[49] Fig. 3 also shows the effect of Ni loading on USY support, and the yield of methane increased with the Ni content on zeolite from 2 to 14%, due to the higher amount of Ni° species after reduction.[48] In conclusion, the amount of Ni loading is dependent on the type of support used. The amount of Ni loading on support will determine its crystallite size and dispersion on the surface of the support.

Effect of second metal on nickel catalyst. It is known that conventional nickel-based catalysts suffer from severe catalyst deactivation in the carbon dioxide methanation reaction, because nickel particles are sintered during the exothermic methanation reaction.[23] To overcome this problem, addition of second metal such as Fe, Zr, Co, La, Y, and Mg has been attempted to enhance the stability and catalytic activity of the nickel-based catalysts.[24,30,32] The addition of a second metal

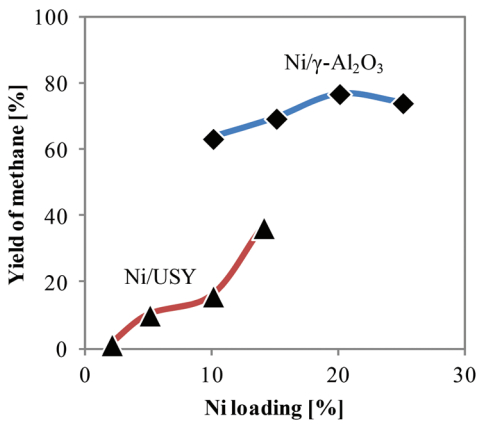

Fig. 3 Effect of Ni loading on yield of methane. For Ni/γ-Al_2O_3 (◆), reaction conditions: reaction temperature = 350 °C, GHSV = 9000 ml g_{cat}^{-1} h, H_2/CO_2 molar ratio = 3.5. For Ni/USY (▲), reaction conditions: reaction temperature = 350 °C, GHSV = 43 000 h^{-1}, $H_2 : CO_2 : N_2$ = 36 : 9 : 10. Results are calculated based on the conversion of CO_2 and selectivity to CH_4 adopted from Graca *et al.* and Rahmani *et al.*[48,49]

(M = Fe, Zr, Ni, Y, and Mg) has been introduced in mesoporous nickel (35 wt%)–M (5 wt%)–alumina xerogel (denoted as 35Ni5MAX) catalysts for methane production from carbon dioxide and hydrogen. In the carbon dioxide methanation reaction, yield for CH_4 decreased in the order 35Ni5FeAX > 35Ni5ZrAX > 35Ni5NiAX > 35Ni5YAX > 35Ni5MgAX. This indicated that the catalytic performance was greatly influenced by the identity of the second metal in the carbon dioxide methanation reaction. The CO dissociation energy and metal–support interaction of the catalyst played key roles in determining the catalytic performance of the 35Ni5MAX catalysts in the reaction, in which the 35Ni5FeAX catalyst retained the most optimal CO dissociation energy and the weakest metal–support interaction, and exhibited the best catalytic performance in terms of conversion of CO_2 and yield for CH_4.[32]

La_2O_3 was used by modification with Ni/SiC as reported by Zhi *et al.*[24] As shown in Fig. 4, It can be seen that CO_2 methanation over Ni–La/SiC begins at 150 °C, while Ni/SiC only becomes active at about 200 °C. The CO_2 conversions of both catalysts have an obvious increase with rising temperature. However, the methane yield of Ni–La/SiC is higher than Ni/SiC at the same temperature. The Ni–La/SiC catalyst also shows better stability than pure Ni/SiC. This is due to the La_2O_3, which can effectively restrain the growth of NiO nanoparticles, improve the dispersion of NiO and strengthen the interaction between NiO and SiC. In addition, La_2O_3 can change the electron environment surrounding the Ni atoms, and thus the reactant CO_2 on the Ni atoms can be activated more easily.[24]

The effect of Fe metal on $NiAl_2O_3$ has been studied by Kang *et al.* for CO_2 methanation.[22] The bimetallic (Ni and Fe) composition in Al_2O_3 was Ni_xFe_{1-x} (x is 0.1, 0.3, 0.5, 0.7 and 0.9) and the results showed that the $Ni_{0.7}Fe_{0.3}/Al_2O_3$ catalyst gave maximum carbon conversion and CH_4 selectivity. Furthermore, the increase of Fe content led to enhancement of the water gas shift reaction and hydrocarbon production.[22] Mg-modified Ni/SiO_2 catalysts with different MgO contents were prepared by impregnation methods.[54] The modification of MgO acted as a key factor in enhancing the capacity of CO_2 adsorption and accelerating the activation of CO_2. Moreover, modified MgO could also increase Ni species dispersion and suppress the metallic Ni sintering and oxidation. The introduction of 1 wt% MgO as a promoter to the 10 wt% Ni/SiO_2 catalyst led to superior catalytic activity and stability (near 100%) at 623 K for 50 h because of the synergistic effect of Ni and Mg species. However, the addition of higher amounts of MgO (2 or 4 wt%) resulted in a slight decrease in catalytic activity due to the blockage of active sites. Therefore, the improved stability and activity of MgO doped Ni/SiO_2 catalysts for CO_2 methanation could be achieved by adding different amounts of MgO.[54] In addition, Guo *et al.* reported that the addition of 4 wt% of Mg on 10 wt% Ni/SiO_2 inhibited the catalytic property of the catalyst significantly due to the low reducibility of the nickel species.[58]

Furthermore, the presence of alkaline-earth metal oxides as a second metal such as SrO on Ni/SiO_2 promoted the catalytic activity and enhanced the catalyst stability.[58] Meanwhile, BaO addition on Ni/SiO_2 enhanced the reaction activity, but the catalyst deactivated significantly after 50 h of time-on-stream due to the sintering of metallic Ni. CaO addition on Ni/SiO_2 affected negligibly the performance of the catalyst.

Co was tested as a second metal in an active oxygen material, the $Ce_xZr_{1-x}O_2$-supported Ni–Co bimetallic nanosized catalyst.[30] The interaction between active metals (Ni and Co) and active oxygen sites in the $Ce_xZr_{1-x}O_2$ support was found to be very important for catalytic performance. Appropriate Co metal addition can improve catalytic stability of catalysts significantly. The active oxygen site of $Ce_xZr_{1-x}O_2$ can improve considerably the catalytic performance due to the presence of more oxygen vacancies.[30] The addition of a proper amount of the VO_x on Ni/treated bentonite improved the catalytic activity of CO_2 methanation.[56] This could be attributed to the enhanced H_2 uptake, increased Ni dispersion, reduced Ni nanoparticle size, and the electronic effect of VO_x that can promote dissociation of CO in the methanation reaction. In the lifetime test of CO_2 methanation under atmospheric pressure, the catalyst was highly stable as it had superior anti-coking and anti-sintering performance compared to the catalyst without the addition of VO_x.

As the discussion above attests, it can be concluded that the presence of a second metal in the Ni catalyst showed a positive effect toward CO_2 methanation. Metals such as Fe, La_2O_3, MgO, Co and VO_x have been used as a second metal on Ni catalysts. They showed a variety of advantages compared to the Ni catalyst. For instance, addition of La_2O_3 on Ni/SiC can restrain effectively the growth of NiO nanoparticles, improve the dispersion of NiO and strengthen the interaction between NiO and SiC. MgO and VO_x plays a key factor in enhancing the capacity of CO_2 adsorption and accelerating the activation of CO_2. Meanwhile, Co metal addition can improve the catalytic stability of catalysts significantly.

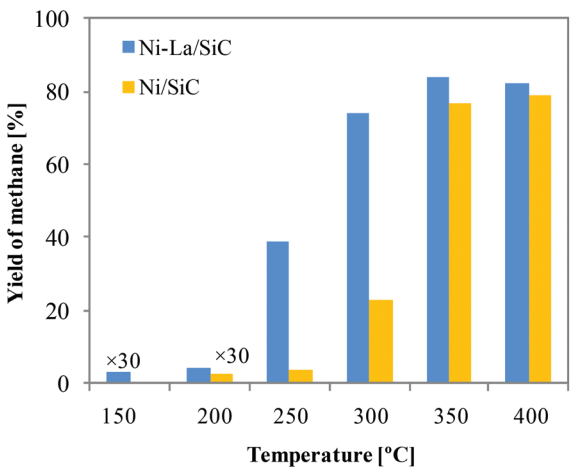

Fig. 4 Catalytic performance of Ni–La/SiC and Ni/SiC under various reaction temperatures. Results are calculated based on the conversion of CO_2 and selectivity to CH_4 adopted from Zhi *et al.*[24]

Effect of preparation method. CO_2 methanation could be affected by the preparation method of the catalyst through the dispersion of active sites. Lu *et al.* has reported a well-dispersed NiO/SBA-15 with high loading prepared by a simple heat treatment (HT) and a conventional solvent impregnation (SI) method.[36] With low NiO loading, the NiO particles were preferentially dispersed on the outer surface of SBA-15 by the HT method. However, with the SI method, the particles preferentially occluded the SBA-15 pores. With high NiO loading, there was no difference caused by the preparation method in the NiO particles location. The preparation method affected the temperature that achieved maximum conversion. The gas conversion increased with increasing NiO loading, regardless of the preparation method. When the NiO loading exceeded 50 wt%, the CH_4 selectivity was 100%. The NiO/SBA-15 by the HT method had high thermal stability under methanation, while by the SI method only the NiO/SBA-15 with high loading had high thermal stability.[36] Zhang *et al.* reported Ni/SiO_2 catalysts prepared by an impregnation method and treated by glow discharge plasma.[38] The results showed that the plasma treatment can improve remarkably the dispersion of active components and enhance the reactivity of Ni/SiO_2 catalysts. The catalytic performance of Ni/SiO_2 in CO_2 methanation is also enhanced by the plasma treatment; the conversion of CO_2 and the space–time yield of CH_4 over the plasma modified catalyst are higher than those over the Ni/SiO_2 catalyst obtained through conventional impregnation and calcination methods.[38] Ni/ceria–zirconia solid solution ($Ni/Ce_xZr_{1-x}O_2$) with Ce and Ni enriched on the surface of the catalysts was prepared *via* a simple, low-cost method as reported by Cai *et al.*[44] The aqueous phase reactions simplify the preparation process, save cost and lead to the enrichment of Ce on the surface of the products. The impregnation method produces Ni enrichment on the surface of the products which enhances the efficiency of the active component. These catalysts exhibit significantly high catalytic performance.[44] The preparation method influenced the rate of reduction of Ni and nucleation of metallic Ni. The degree of interaction between Ni and the support also depends on the preparation route of the catalyst. Therefore, on the basis of the reports above, the method of catalyst preparation can be a vital factor to improve CO_2 methanation. Based on overall discussion of Ni catalysts, the current catalysts used for CO_2 methanation are summarized in Table 1.

Noble metal-based catalysts

The hydrogenation of CO_2 to methane has been investigated over Ru catalysts on different supports.[40,67–69,70–75] Ruthenium is believed to be even more active in CO_x methanation than nickel, but is also considerably more expensive.[76] In contrast to Ni, which may be deactivated at low temperatures due particle sintering, interaction of the metal particles with carbon monoxide, formation of mobile nickel subcarbonyls and formation of carbon deposits.[77,78] Instead, ruthenium catalysts have been reported to be the most stable when operating over

Table 1 Summary of various Ni catalysts for CO_2 methanation

Catalysts	Preparation method	Ni (nm)	T [°C]	X_{CO_2} [%]	S_{CH_4} [%]	Stability test, conversion [%]	Ref.
12 wt% Ni/ZrO_2–Al_2O_3	Impregnation-precipitation	5.4 (6.3)[a]	360	69.8	100	Decreased by 1.6% after 100 h	21
5 wt% Ni–$Ce_xZr_{1-x}O_2$	Pseudo sol–gel	20.8 (39)[a]	350	80	>98	Decreased by 18.8% after 140 h	23
15 wt% Ni–La/SiC	Impregnation	8.3 (8)[a]	360	85	100	Stable after 70 h	24
10 wt% Ni/CeO_2	Impregnation	17[b]	350	93	100	n/a[d]	26
10 wt% Ni/β-zeolite	Impregnation	25.8	360	97	n/a	n/a	31
10 wt% Ni/β-zeolite-with plasma	Impregnation	18.7[b]	240	94	n/a	n/a	31
35 wt% Ni/5 wt% Fe/Alumina xerogel	Single step sol–gel	7.39	220	63.4	99.5	n/a	32
5 wt% Ni/ceria-zirconia	Pseudo sol–gel	21	350	67.9	98.4	Decreased by 15% after 90 h	33
5 wt% Ni/2 wt% ceria/Al_2O_3	Co-impregnating boehmite with metal solutions		300	70	100	Stable after 120 h	34
15 wt% Ni/TiO_2	Precipitation–deposition	2.1[c]	260	96	99	Decreased by 2.9% after 81 h	35
70 wt% Ni/SBA-15	Heat treatment	n/a	300–450	99.2	100	High thermal stability due to unchanged surface area after catalytic test.	36
Ni/SiO_2	Impregnation method and treated by glow discharge plasma (H_2 atmosphere)	n/a	250	90	~100	Decreased by 15.54% after 100 h	38
20 wt% Ni/H–Al_2O_3	*In situ* reduction of a hierarchical $Ni^{II}Al^{III}$-LDH precursor at reduction temperatures of 400 °C	5–8.1[c]	300	99	>99	Decreased by 7% after 252 h	39
5 wt% Ni–$Ce_xZr_{1-x}O_2$	Hydration-impregnation	n/a	420	75.66	>80	Decreased by 15% after 60 h	44
14 wt% Ni/USY	Impregnation	n/a	400	65.5	94.2	Stable after 10 h	48
20 wt% Ni/nanocrystalline γ-Al_2O_3	Impregnation	18.9	350	78	100	Stable after 600 min	49

[a] Used catalyst; determined by Sherrer formula. [b] After reduced at 600 °C; determined by Sherrer formula. [c] Determined by TEM. [d] n/a: not available.

a wide range of temperatures.[75] Sharma *et al.* studied the methanation of CO_2 on ceria doped with Ni, Co, Pd, or Ru. $Ce_{0.96}Ru_{0.04}O_2$, and $Ce_{0.95}Ru_{0.05}O_2$ performs best, converting 55% of CO_2 with a 99% selectivity for methane, at a temperature of 450 °C.[68] They found that the methanation reaction takes place on the reduced $Ce_{0.95}Ru_{0.05}O_2$, and the role of the Ru dopant is to make the reduction possible at lower temperatures than on pure ceria.[68] The catalytic conversion of CO_2 to CH_4 on cobalt oxide and Ru-doped cobalt oxide nanorods was studied by Zhu *et al.*[71] The active phases of the two catalysts are metallic cobalt and bimetallic Co–Ru, respectively. As presented in Fig. 5, the yield of CH_4 on the Ru-doped cobalt oxide is obviously enhanced by formation of a bimetallic Co–Ru ultrathin film in its surface region in contrast to that of cobalt and Ru/SiO_2 catalyst in the temperature range of 200–340 °C. These comparisons indicate that the surface of the active phase of Ru-doped catalyst is bimetallic Co–Ru instead of pure Co or pure Ru.[71] Recently, Upham *et al.* found that the activity of $Ru_{0.05}Ce_{0.95}O_x$ is sensitive to the degree of surface reduction. They found that if a surface is too reduced (*i.e.* it has too many oxygen vacancies) or too oxidized, its performance is poor.[75]

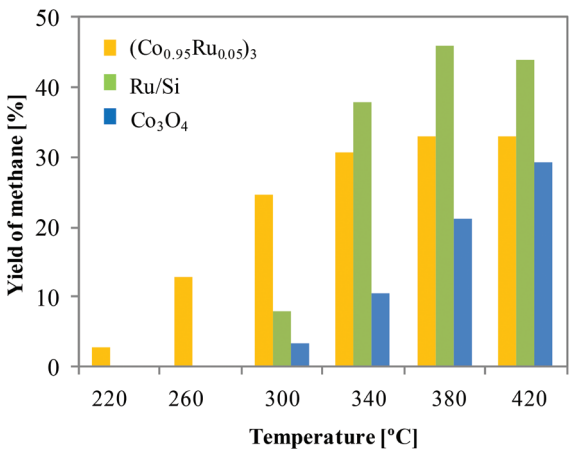

Fig. 5 Catalytic performances of Co_3O_4, $(Co_{0.95}Ru_{0.05})_3O_4$ and Ru/SiO_2. The measurements of catalytic conversion and selectivity were performed in a fixed-bed microreactor at 50 mL min^{-1} flow rate, 1 bar reactant pressure, and a reactant mixing ratio $CO_2 : H_2 = 1 : 4$. The weight of catalyst is 100 mg. Ru is 5 wt% of SiO_2. Results are calculated based on the conversion of CO_2 and selectivity to CH_4, adapted from Zhu *et al.*[71]

The effect of Ru loading on zeolites was studied on CO/CO_2 methanation.[73] Increasing the Ru loading causes an increase of the mean particle size from 0.9 nm (2.2 wt% Ru) to 1.9 nm (5.6 wt% Ru). At the same time, the activity for CO methanation also increases, while the selectivity for CO methanation, which is constant at 100% for reformate gases with 0.6% CO, decreases at low CO content. The latter findings are interpreted in terms of a change in the physical effects governing the selectivity for CO methanation with increasing Ru particle size, from an inherently low activity for CO_2 dissociation and subsequent CO_{ad} methanation on very small Ru nanoparticles to a site-blocking mechanism on larger Ru nanoparticles. In the latter mechanism, CO_2 methanation is hindered by a reaction-inhibiting adlayer of CO at higher CO_{ad} coverages, *i.e.*, at not too low CO concentrations, but facile in the absence of a CO adlayer, at lower CO concentrations in the reaction gas mixture.[73] Table 2 illustrates the summary of various Ru catalysts for CO_2 methanation. The Ru loading and/or the size of metal cluster is an important factor for the high activity of CO_2 methanation. The introduction of Ru metal promoted the reduction of cerium oxide at lower temperatures.

Hydrogenation of CO_2 toward methane has been extensively study using supported rhodium catalysts.[12,27,79–83] The methanation of CO_2 at low temperature (between 50 and 150 °C) and pressure (2 bar) was performed on Rh/γ-Al_2O_3 catalyst in a pulse reactor and performed with 100% selectivity to methane.[12] The oxidation state of the Rh plays an important role in the distribution of the adsorbed species on the catalysts: the *gem*-dicarbonyl species are more reactive than the Rh–CO linear species. The preferential formation of these species will be the origin of the difference in the reactivity of CO_2 and CO. Oxygen, in low amounts, has a positive effect on the methanation while CO inhibits the methanation of CO_2.[12]

Karelovic and Ruiz studied the effect of metal particle size on the performance of CO_2 methanation over Rh/γ-Al_2O_3 catalysts.[79] Catalysts with varying Rh content gave rise to different Rh particle sizes (between 3.6 and 15.4 nm). In the condition studied, selectivity to methane was 100% over the entire range of temperature and Rh loading studied. The intrinsic activity of Rh/γ-Al_2O_3 catalysts in CO_2 hydrogenation to methane was found not to depend on particle size at temperatures between 185 and 200 °C, whereas at lower temperatures larger particles favored higher activity.

Table 2 Summary of various Ru catalysts for CO_2 methanation

Catalysts	Preparation method	T [°C]	X_{CO_2} [%]	S_{CH_4} [%]	Highlight	Ref.
$Ce_{0.95}Ru_{0.05}O_2$	Combustion	450	55	99	The methanation reaction takes place on the reduced $Ce_{0.95}Ru_{0.05}O_2$, and the role of the dopant (Ru) is to make the reduction possible at lower temperatures than on pure ceria	68
35Ni5Fe0.6RuAX	Single-step sol–gel	220	68.2	98.9	Optimal ruthenium content was required for the maximum production of methane from carbon dioxide and hydrogen	40
$(Co_{0.95}Ru_{0.05})_3O_4$ nanorod	Modified wet chemistry	380	33	97	Active phases of the two catalysts are metallic cobalt and bimetallic Co–Ru, respectively	71

The mechanical mixtures of Rh/γ-Al_2O_3 and Ni loaded activated carbon (AC) catalysts, show a significant catalytic synergy in the methanation of CO_2.[27] This effect is more important when the content of Ni is 1 wt%. The production of methane over the mixed catalyst is higher compared with the methane formation observed with individual catalysts. This synergy is explained by cooperation between the two catalysts during methanation. Particularly, 1 wt% Rh/γ-Al_2O_3 is highly efficient at CO_2 adsorption. On the other hand, a 1 wt% Ni/AC catalyst is able to absorb a high quantity of hydrogen and very little carbon dioxide. These properties, joined together by a simple mixed catalyst, induce an increase of carbon dioxide conversion and methane formation. In all cases only methane is formed. The augmentation of the catalytic performances could be attributed to a migration of activated hydrogen species from 1 wt% Ni/AC catalysts toward 1 wt% Rh/γ-Al_2O_3. This hydrogen can then react with CO_2 species to form methane but also to preserve rhodium particles in an adequate reduced state essential for CO_2 hydrogenation.

CO_2 methanation at low temperature and atmospheric pressure was also studied over Rh/TiO_2 catalysts.[80] Catalysts with different Rh contents (0.5–5 wt%) were prepared in order to obtain different mean cluster sizes. The rate of methane production per surface Rh atom increases as metal particle size increases up to *ca.* 7 nm. Beyond this size, the rate does not change appreciably. Higher activation energies (up to 28.7 kcal mol^{-1}) are obtained for catalysts with small cluster size (*ca.* 2 nm), whereas for larger particles (>7 nm), the activation energy is lower and does not change with size (*ca.* 17 kcal mol^{-1}). The authors of ref. 80 proposed that smaller Rh particles tend to bind the CO(ads) intermediate more strongly than larger ones. The activation energy for the dissociation of adsorbed CO species does not vary with Rh particle size, which suggests that smaller particles are not intrinsically less-active, but they present less active-sites than larger ones. The study of the kinetic parameters permits the proposal that CO(ads) dissociation is aided by the presence of H species and that a likely surface intermediate is Rh carbonyl hydrides.[80]

Recently, Beaumont *et al.* has reported the role of Pt nanoparticles (Pt NPs) in Co–Pt/SiO_2 on the methanation of CO_2.[83] The presence of Pt NPs deposited near Co NPs (within the same mesoporous oxide support) can enhance the CO_2 methanation rate by up to a factor of 6 per Co surface atom. The Pt NPs were also able to enhance reduction of Co at temperatures relevant to CO_2 methanation. The hydrogen atoms dissociated on Pt may be transferred to the Co NPs *via* long-distance hydrogen atom spillover, aiding their reduction.

Pd/Al_2O_3 and Pd/MWCNT were investigated as bifunctional catalysts for CO_2 methanation and their role as atomically dispersed metal centers in overall catalytic performance were discussed by Kwak *et al.*[72] The results of this study clearly show that atomically dispersed supported metals can be catalytically active even in the demanding reaction of CO_2 reduction. Their activity and selectivity patterns, however, differ by a large extent from those of 3D metal particles. The CO_2 hydrogenation reaction on Pd/Al_2O_3 and Pd/MWCNT catalysts have unambiguously proven the need for two different functionalities in an active catalysts. In the 1% Pd/MWCNT catalyst, Pd (present in atomic dispersion) can activate H_2, but the functionality to activate CO_2 is absent. Therefore, this material is inactive in the reduction of CO_2 with H_2. In the other two systems, which also contain Pd in atomic dispersion but in the presence of oxide components (0.5% Pd/Al_2O_3 and 1% Pd + 2.3% La_2O_3/MWCNT), the reduction of CO_2 proceeds at high rates. This is due, most probably, to the concerted reaction between the oxide-activated CO_2 and the metal-activated hydrogen. However, the reduction of CO_2 in these two systems produces primarily (or almost exclusively) CO, and not CH_4. This is the consequence of the absence of Pd metal clusters where the initially formed CO could be activated. The CO that forms from the oxide-activated CO_2 desorbs from these catalysts and is detected in the effluent. However, when Pd clusters are present in the system (10% Pd/Al_2O_3) the initially formed CO can be readily hydrogenated to CH_4 on the metal particles (both adsorbed CO and atomic hydrogen present on the metal clusters). The mechanism is presented clearly in Fig. 6. Therefore, the methane selectivity over the catalyst that contain large metal clusters is high. The results obtained show clearly that the oxide support material, even when it is considered inert like Al_2O_3, can function as a critical, active component of complex catalyst systems.

Shape-controlled Pd nanocubes and nanopolyhedra particles embedded in mesoporous silica shells were studied for CO_2 hydrogenation.[84] The catalysts were compared to Pd/SiO_2 prepared by wetness impregnation and it was found that the Pd/SiO_2 exhibits a strong deactivation. Meanwhile, the activity of both embedded solids is remarkably stable. This difference is due to a significant Pd particle sintering in the SiO_2, while no increase of particle size is observed for the core@shell solids.[84]

Supported gold, rhodium and bimetallic rhodium-core–gold-shell catalysts were studied on CO_2 methanation.[81] The supports used were titanate nanotubes and nanowires. The gold particles were highly dispersed besides the metallic form on all supports. The main product of CO_2 hydrogenation was CH_4 on all catalysts. IR spectra revealed the existence of CO and formate species on the surface. In addition, a new band was observed around 1770 cm^{-1} which was assigned as tilted CO, which is bonded to Rh and interacts with a nearby oxygen vacancy of the support.[81]

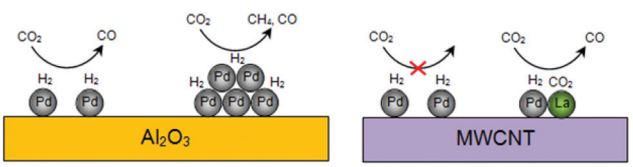

Fig. 6 Mechanisms of various catalysts for CO_2 methanation. The results show the importance of different functionalities in an active catalyst (*i.e.*: Al_2O_3 as a metal oxide support and Pd in a metal cluster).[72]

Other metal-based catalysts

Instead of Ni and noble metal-based catalysts, other metals such as Co,[85–89] and Mg[50] were also tested to determine the potential of those metal catalysts for CO_2 methanation. Srisawad *et al.* reported Co/Al_2O_3 catalysts prepared by the solid-state reaction between gibbsite and various cobalt salts such as cobalt acetate (CoAc), cobalt acetylacetonate, cobalt chloride, and cobalt nitrate (CoNT) for the hydrogenation of carbon dioxide.[85] Compared to the catalysts prepared by conventional impregnation of an aqueous solution of cobalt nitrate on alumina (CoNTImp), the solid-state catalysts (CoNT and CoAc) exhibited much higher activity for CO_2 hydrogenation with comparable CH_4 and CO selectivity. Unlike the impregnation catalysts, in which most of the Co_3O_4 particles/clusters were located deep inside the pores of alumina, the solid-state reaction resulted in the dispersion of cobalt oxides mostly on the external surface of alumina. As a consequence, CO_2 adsorption and dissociation to adsorbed CO and O (the initial steps in CO_2 hydrogenation) were not limited by the slow diffusion of CO_2, so a high CO_2 hydrogenation activity was obtained. The average crystallite size of Co_3O_4 and the metal–support interaction depended on the cobalt precursor used during the solid-state synthesis. Nevertheless, the solid state reaction of gibbsite and cobalt chloride at 650 °C resulted in very poor CO_2 hydrogenation activity due to the formation of inactive cobalt aluminate.[85]

Mesoporous Co/KIT-6 and Co/*meso*-SiO_2 catalysts with well-dispersed Co species were reported by Zhou *et al.* for CO_2 methanation.[86] The Co/KIT-6 catalyst has a large specific surface area (368.9 $m^2\ g^{-1}$) and a highly ordered bicontinuous mesoporous structure. The Co/KIT-6 exhibits excellent CO_2 catalytic hydrogenation activity and methane product selectivity, which are both higher than those of the Co/*meso*-SiO_2 catalyst at high reaction temperatures. The high dispersion of the Co species and the large specific surface area of the prepared Co based catalysts contribute to the high catalytic activities. In addition, the highly ordered, bicontinuous, mesoporous structure of the Co/KIT-6 catalyst improves the selectivity for the methane product.[86]

A model of cobalt catalysts for CO_2 hydrogenation prepared using colloidal chemistry was studied by Iablokov *et al.*[88] The turnover frequency at 6 bar and at 200–300 °C increased with cobalt nanoparticle size from 3 to 10 nm. They demonstrated that near-monodisperse nanoparticles in the size range of 3–10 nm could be generated without using trioctylphosphine oxide.[88] Different supports, such as SSP, MCM-41, TiSSP and TiMCM were used to prepare Co catalysts for CO_2 hydrogenation for methanation.[89] It is found that after calcination of the catalysts, Ti is present in the form of anatase. The introduction of Ti plays an important role in the properties of Co catalysts by: (i) facilitating the reduction of Co oxides species which interact strongly with the support; (ii) preventing the formation of silicate compounds; and (iii) inhibiting the RWGS reaction. Based on CO_2 hydrogenation, the CoTiMCM catalyst exhibits the highest activity and stability.[89]

An alumina supported cobalt oxide based catalyst doped with platinum prepared by the wet impregnation method for CO_2 methanation was reported by Bakar *et al.*[45] The catalyst showed an excellent activity with 70.1% of CO_2 conversion into methane and 47% of CH_4 formation at the maximum temperature studied of 400 °C. This catalyst possessed the active site Co_3O_4 in the face-centered cubic form and PtO_2 in the orthorhombic phase with Al_2O_3 existing in the cubic phase.[45]

Recently, alumina-supported Co_4N catalysts prepared by the NH_3-temperature programmed reaction (NH_3-TPR) were used to perform CO_2 methanation in a fixed bed reactor.[87] The activity results revealed that Co_4N was a superior active phase for CO_2 conversion compared to Co^0. The formation of a Co_4N phase led to a strong metal–support interaction modulating the metal particle size and dispersion. The addition of N to form cobalt nitride greatly improved the overall adsorption capacity of the catalyst. Moreover, a 250 h stability test demonstrated that the γ-Al_2O_3-supported Co_4N catalyst had excellent resistance to coking and metal sintering. This superior long-term performance could be related to the increased surface basicity and stronger Co_4N–γ-Al_2O_3 interaction.

In the search for novel methanation catalysts, hydrogen storage alloys might be an alternative to classical catalysts for CO_2 methanation. Compared to MgH_2 and other Mg based alloys, *e.g.* Mg–Al or Mg_2Cu, Mg_2Ni exhibits a fast activation under reducing conditions for the surface layers. Therefore, Kato *et al.* has studied the potential of the Mg–Ni hydride (Mg_2NiH_4) alloy for CO_2 methanation.[50] The Mg_2NiH_4 was investigated with respect to the catalytic property of the hydride surface for CO_2 methanation. The formation of surface oxide layers hinders the decomposition of the hydride. The surface oxidation is accompanied by segregation of Mg oxides and Ni at the disproportionated surface on Mg_2NiH_{4-x}. However, the active Ni sites at the surface are associated with the ready dissociation of hydrogen molecules and subsequent hydrogenation of intermetallic Mg_2Ni. The simultaneous precipitation of Ni-clusters is attributed to the catalytic activity of the hydride surface, *i.e.* for dissociative adsorption of CO_2 molecules and their subsequent hydrogenation. As the Ni particles are formed during decomposition, the modified surface becomes more active for CO_2 methanation.

A summary of Co catalysts is illustrated in Table 3. Previous studies showed that Co catalysts have a specific catalyst preparation before being used on CO_2 methanation. Among the promising techniques of catalyst preparation are solid-state reactions, colloidal chemistry and NH_3-temperature programmed reactions. These technique showed superior catalytic activity compared to the conventional impregnation method. The dispersion of cobalt oxide on the external surface plays an important factor for the high activity of reaction and this can be achieved *via* a specific technique such as solid-state reaction. Meanwhile, alloy-based catalysts such as Mg–Ni hydride can be potentially used for CO_2 methanation due to their fast activation of CO_2 under reducing conditions.

Table 3 Summary of various Co catalysts for CO_2 methanation

Catalysts	Preparation method	T [°C]	X_{CO_2} [%]	S_{CH_4} [%]	Ref.
Co/Al_2O_3	Mechanical mixture of cobalt nitrate and gibbsite	270	76	82.2	85
Co/KIT-6	Impregnation	260	46	100	86
Co/*meso*-SiO_2	Impregnation	360	30	100	86
Co/SSP	Impregnation	220	27	89.5	89
Co/MCM	Impregnation	220	28	91.4	89
Co/TiSSP	Impregnation	220	16	92.1	89
Co/TiMCM	Impregnation	220	34	94.9	89
Co_4N/γ-Al_2O_4	NH_3-temperature programmed reaction	350	99	98	87
Co/γ-Al_2O_4	Impregnation	350	79	n/a[a]	87

[a] n/a: not available.

Reaction mechanism

Although the methanation of CO_2 is a comparatively simple reaction, its mechanism appeared to be difficult to establish. Presently, there are still arguments on the nature of the intermediate compound involved in the process and on the methane formation scheme. The reaction mechanisms have been classified into two main categories. The first one involves the conversion of CO_2 to CO prior to methanation and the subsequent reaction follows the same mechanism as CO methanation.[12,79] The other reaction mechanism involves the formate species as the main intermediate during the reaction.[33] Note that, even for CO methanation, there is still no consensus on the kinetics and mechanism. It has been proposed that the rate-limiting step is either the formation of the intermediate CH_xO and its interaction with hydrogen or the formation of surface carbon in CO dissociation and its hydrogenation.[90]

Numerous studies have been conducted on the adsorption and activation of CO_2 on metal surfaces such as Cu,[91] Pt,[92] Pd,[93] and Fe[91] where the Fe(110) surface has been identified to be most suitable for CO_2 activation.[94] This has been attributed to a remarkable charge transfer (0.83 e−) from the surface to the CO_2 molecule and to the elongation of one of the C–O bonds (to *ca.* 1.30 Å) including bending of the CO_2 molecule.[94] The most widely used metals for CO_2 methanation, however, are Ni, Ru and Rh. Using density functional theory (DFT) calculations, it has been verified that the reaction on Ni also involves the formation of the bent CO_2 intermediate.[95]

The findings on the fundamental insight into the CO_2 adsorption mechanism on CeO_2 has been explored by Hahn *et al.*[96] They employed the functional theory to study the adsorption of carbon dioxide on CeO_2(111). At low coverage (1/9 monolayer), CO_2 is found to adsorb preferably in a monodentate configuration forming a carbonate species with a surface O atom. In this configuration, the CO_2 molecule is bent with an O–C–O angle of 129° and a remarkable elongation (to 1.27 Å) of the C–O bond length compared to the gas phase molecule, indicating a high degree of CO_2 activation. A similar activation is observed when the CO_2 molecule adsorbs as bidentate carbonate; however, this configuration is less stable. Linear configurations are found to adsorb very weakly at low coverage by physisorption. Increasing the coverage leads to a decrease of the stability of mono- and bidentate configurations which can be attributed to repulsive interactions between adjacent adsorbates and the limited capacity of the CeO_2(111) surface to donate electrons to the adsorbates. In contrast, the binding energy of linearly adsorbed CO_2 is shown to be coverage independent. At coverages >1/4 monolayer, the stable mixed configurations of monodentate, bidentate, and linear species are present simultaneously on the surface. The most stable configurations are found when 1/3 monolayer CO_2 is bound as monodentate species, and additional molecules are physisorbed forming partial layers of linear species. Analysis of the projected density of states has shown that the orbitals of linear species in the first partial layer lie at lower energies than the ones of the second partial layer, suggesting stabilization of the former through interactions with preadsorbed monodentate species.[96]

DFT calculations have also been performed to understand the complete hydrogenation mechanism for CO_2 on Ni(110) surfaces.[46] The calculations show that CO_2 hydrogenation passes *via* various stable intermediates, namely, carbon monoxide, methoxy and formate, and yields the product methane. It is suggested that the methane formation *via* hydroxyl carbonyl intermediate requires a lower energy barrier than *via* carbon monoxide and formate intermediates on the Ni(110) surface.

The mechanism of CO_2 methanation on a Ni/$Ce_{0.5}Zr_{0.5}O_2$ catalyst has been investigated using *in situ* FTIR spectroscopy.[47] It was proposed that CO_2 prefers to adsorb on surface oxygen sites adjacent to Ce(III) compared with those adjacent to Ce(IV)/Zr or surface hydroxyl sites. Five adsorption species were revealed for CO_2 adsorption on Ni/$Ce_{0.5}Zr_{0.5}O_2$. The adsorption sites and resulting species are as follows: (1) the surface oxygen sites adjacent to Ce(IV) or Zr resulting in monodentate carbonates; (2) the surface oxygen sites adjacent to Ce(III) which are connected with an oxygen vacancy resulting in monodentate carbonates; (3) the surface oxygen vacancy adjacent to Ce(III) resulting in bidentate carbonates; (4) the surface oxygen vacancy adjacent to Ce(IV) resulting in bidentate carbonates; (5) the surface hydroxyl sites of Ce(IV) or Zr resulting in hydrogen carbonates. It was found that monodentate carbonates on Ce(III) are easier to be hydrogenated than those on Ce(IV). Formate species were found to be the main intermediate species during the reaction and Ce(III) sites were proposed to be active sites for their hydrogenation. A reaction mechanism that could account for all of these observations is presented in Fig. 7.

Hydrogen carbonates and carbonates are sourced from CO_2 adsorption on surface hydroxyls and the surface oxygen sites in the cerium–zirconium solid solution, respectively. Since the bidentate carbonates are not stable enough to be hydrogenated to formate species, the formate species are derived from the hydrogenation of hydrogen carbonates and monodentate carbonates. Although the hydrogen that adsorbs on the surface oxygen of $Ce_{0.5}Zr_{0.5}O_2$ could convert carbonate to formate,

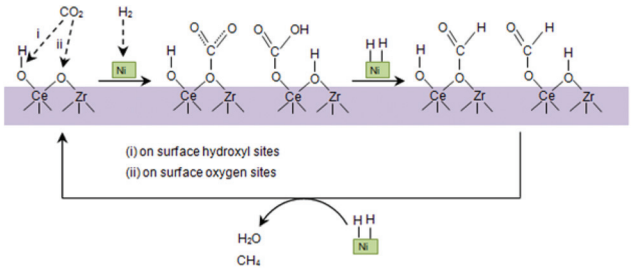

Fig. 7 Proposed reaction pathways for CO_2 methanation on a Ni/$Ce_{0.5}Zr_{0.5}O_2$ catalyst. Adopted from Pan *et al.*[47]

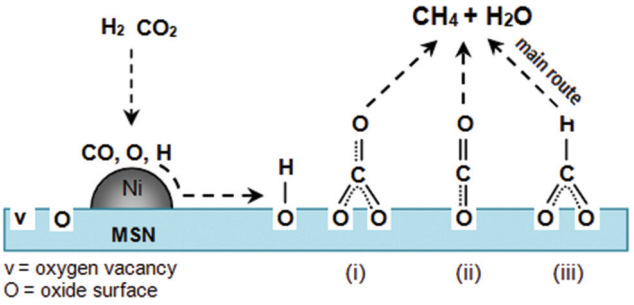

Fig. 8 Plausible mechanism of CO_2 methanation on Ni/MSN; (i) bridged carbonyl, (ii) linear carbonyl and (iii) bidentate formate. Adopted from Aziz *et al.*[42]

nickel particles still play an important role in the dissociative adsorption of hydrogen. The subsequent hydrogenation reactions of formate using metal adsorbed hydrogen atoms lead to the formation of $-CH_2OH$. The $-CH_2OH$ species are then hydrogenated to $-CH_3$ and CH_4.[47]

Aldana *et al.* has studied the methanation of CO_2 over Ni–$CZ_{sol-gel}$ and Ni–silica.[33] The results show that the Ni–$CZ_{sol-gel}$ catalysts have much better activity compared to Ni–silica. The mechanism of CO_2 methanation over Ni–$CZ_{sol-gel}$ explains the involvement of weak basic sites of the support for the adsorption of CO_2 and implies a stable metal–support interface. The mechanism for CO_2 methanation on the studied Ni–$CZ_{sol-gel}$ catalyst is proposed. The main reaction pathway does not involve CO as an intermediate. Carbon dioxide adsorbs on sites of mild basicity to form covalent carbonates, hydrogen carbonates and then bidentate carbonates. These species are further reduced and hydrogenated by H atoms formed by dissociation of hydrogen at the surface of Ni° particles to form formates and then probably formaldehyde-type and methoxy species (not observed) and to finally release methane. A parallel pathway may exist where CO is formed by a redox cycle on reduced ceria. This pathway may decrease activity by CO–H_2 competitive adsorption on metal particles and enhance deactivation by Ni sintering through the formation of di- or tricarbonyls and by the formation of stable polycarbonates which block the CO_2 adsorption sites.

Nickel promoted mesostructured silica nanoparticles (Ni/MSN) were highly active for CO_2 methanation due to the presence of intra and interparticle pores which led to an increase in the number of oxygen vacancies in the catalyst.[41–43] The presence of oxygen vacancies in Ni/MSN is necessary to explain the formation of surface carbon species, C(a). It is possible that a C(a) species could interact directly with an oxygen vacancy in MSN. The role of Ni sites in MSN may be to dissociate hydrogen to form atomic hydrogen, in which atomic hydrogen facilitates the formation of methane. However, the later findings on Ni/MSN reported that the Ni was also responsible for the dissociation CO_2 to CO and CO.[42] As presented in Fig. 8, firstly, CO_2 and H_2 was adsorbed onto metal sites, followed by dissociation to form CO, O and H atoms, and migration onto the MSN surface. The CO then interacted with oxide surfaces of the MSN to form bridged carbonyl and linear carbonyl. Bidentate formate was also formed through the interaction with atomic hydrogen. Meanwhile, the O atom spilt over onto the surface of the MSN and was stabilized in the oxygen vacancy site near the metal site. The adsorbed oxygen then reacted with atomic hydrogen to form hydroxyl on the MSN surface in which a further reaction with another atomic hydrogen formed a water molecule. Finally, the adsorbed carbon species was further hydrogenated to methane and another water molecule. In the study, all three species (linear carbonyl, bridged carbonyl and bidentate formate) could be an intermediate for CO_2 methanation as reported by previous studies.[33,47,82,97–99] However, the bidentate formate species could be the main intermediate for CO_2 methanation in agreement by the previous studies.[33,47,97]

Two plausible reaction paths were found for the transformation of CO_2 to CH_4 on TiO_2-supported Ru nanoparticles by density functional theory (DFT) using the generalized gradient approximation with periodic boundary conditions.[74] CO_2 adsorbs with a bent structure on the modeled Ru cluster supported on the TiO_2 (10 1) surface. Two plausible sites for CO_2 adsorption were found through the optimized structure: the top and the side of the Ru cluster. The CO_2 molecule is readily adsorbed at both adsorption sites of the Ru cluster at moderate temperature, and the adsorbed CO_2 to the Ru cluster is more stable than to the Ru surface. This result is caused by the difference of the Ru structure between the Ru surface and the Ru nanoparticles. The adsorbed CO_2 on each site transforms into CO through different reaction paths, but the potential energy barriers for each reaction path are almost the same. Both adsorption sites, therefore, function as active sites of the transformation of CO_2 to CO at moderate temperature. It is possible for the elementary reactions of the hydrogenation of adsorbed CO and of the production of CH_4 to become the rate-determining steps over the methanation reaction, because these two reactions have a higher potential energy barrier than that of other elementary reactions in the overall reaction path. These potential energy barriers for the hydrogenation of CO and the production of CH_4 on TiO_2-supported Ru nanoparticles were lower than those on the bulk Ru surface, which explains the high activity of the Ru nanoparticle-loaded TiO_2 catalyst. The lowering of these potential energy barriers can be caused by weak charge transfer between Ru atoms and

adsorbed species on the TiO_2-supported Ru nanoparticles. The electron charge transfer from CO to the adsorbing Ru atoms on Ru/TiO_2 was less than that on the Ru surface, indicating that the interaction between the adsorbed species and Ru atoms on Ru/TiO_2 was weaker. Therefore, the adsorption of CO and CH_3 on Ru/TiO_2 is less energetically favorable than on the Ru slab, and thus the potential energy barriers of the hydrogenation reaction of CO and the production of CH_4 are smaller.[74]

Panagiotopoulou *et al.* has reported the mechanism of methanation of CO_2 over 5% Ru/TiO_2 through *in situ* FTIR spectroscopy (DRIFTS) and transient mass spectrometry techniques.[70] It is shown that interaction of the prereduced catalyst with the reaction mixtures results in the development of various Ru-bonded carbonyl species on reduced and partially oxidized sites as well as on sites located at the metal–support interface. The nature and population of these species depend strongly on feed composition and reaction temperature. The reaction dominates at lower reaction temperatures which involves hydrogenation of surface carbon produced by dissociative adsorption of CO, whereas the latter involves hydrogenation of CO species adsorbed at the metal–support interface.

At low temperatures, typically <250 °C, dissociation of CO results in accumulation of adsorbed oxygen species which cannot be removed from the catalyst surface, rendering it inactive. Catalytic activity is restored at higher temperatures, where partially oxidized sites are reduced efficiently by adsorbed hydrogen atoms. The associative reaction pathway is the only one which is operable under conditions of CO_2 methanation and proceeds *via* intermediate formation of carbonyl species at the metal–support interface, produced by the RWGS reaction.

A comparison of the reaction mechanism between Ni and Ru-based catalysts is presented in Table 4. It can be concluded that many researchers agreed that the formate species on Ni catalyst could be a main intermediate or precursor to the formation of methane. However, the Ni catalyst may deactivate due to the formation of di- or tri-carbonyls and stable polycarbonates which block the CO_2 adsorption sites. In contrast, the carbonyl species is of importance for Ru catalysts. This species may form on metal and/or metal–support interfaces. The nature and population of intermediate species for Ru catalysts is strongly dependent on feed composition and reaction temperature (moderate temperature).

Summaries and future prospects

Global warming has pushed the necessity to reduce the emission of gases responsible for the greenhouse effect, mainly CO_2, caused by the use of fossil fuels. The increasing amount of CO_2 in the atmosphere is causing climate change on a global scale. Therefore, a reduction in CO_2 emission into the atmosphere is an urgent necessity. However, the levels of CO_2 are increasing with increase in the world's population and improvement in living standards. Although various physical and chemical techniques have been proposed for the fixation of exhausted CO_2, such as fixation in carbonates, geological or ocean storage, or afforestation, their immediate practical application has drawbacks in terms of economic factors, safety, efficiency, and reliability. The use of CO_2 as a renewable and environmentally friendly source of carbon is a highly attractive approach.

Research direction

Various strategic considerations, technical approaches, and specific research directions have been presented for the methanation of CO_2. The prevalent view of the active site is the synergy between the primary catalyst and support or promoter. Because the catalyst for CO_2 methanation is sensitive to the structure of the catalyst, the preparation method, preparation conditions and the component significantly influence its performance. In summary, future research directions on catalysts for CO_2 methanation are proposed as follows:

1. To explore further new materials and optimize the catalyst synthesis conditions in order to achieve high activity and stable Ni catalysts with low reaction temperature of CO_2 methanation.

2. To explore high surface area mesoporous materials with tunable pore size to improve catalyst structures for the purpose of achieving higher volumetric surface areas. For example, the

Table 4 Comparison of reaction mechanism between Ni and Ru-based catalyst

Catalysts	H_2 adsorption sites	CO_2 adsorption sites	Intermediate species	Comments	Ref.
Ni-based	Reduced Ni	• Reduced Ni • Oxygen vacancy	• Monodentate carbonates at support surface • Bidentate carbonates at support surface • Bidentate formates at support surface (main intermediate)	The formation of di- or tri-carbonyls and stable polycarbonates block the CO_2 adsorption sites and these will lead to deactivation of Ni catalyst	33,42,47
Ru-based	Reduced Ru	• Reduced Ru • Partially oxidized Ru • Oxygen vacancy	• Carbonyl species at the metal–support interface • Carbonyl species at the metal surface	The nature and population of intermediate species depend strongly on feed composition and reaction temperature	70,74

exploration of innovative synthesis methods to produce a high surface area of mesoporous cerium oxide and/or hybrid catalysts of cerium with mesoporous material.

3. To explore a new way to generate or tailor the basic sites of the catalyst. For example, by incorporation of specific amount of metal chloride or alkali metal on the catalyst support.

4. To improve catalyst stability, for example, by exploring alternative metals other than nickel and/or enhancing the basicity of the catalyst by adding an alkaline earth metal (*i.e.*: La_2O_3) as a promoter.

5. To understand fundamentally the mechanisms of CO_2 methanation and explore its relationship with catalyst active site structures using both theoretical calculations (molecular/electronic level modeling) and experimental approaches to tailor new catalyst structures.

Presently, it can be suggested that Ni is the most suitable metal in terms of activity and an economic point of view. Therefore, Ni catalysts have the potential to be used widely in industrial processes. The high surface area of the support is crucial for the methanation reaction which promotes high dispersion of the metal or active phase on the surface of the catalyst support. High surface area materials such as MSN and MOFs are among the best candidates that exhibited high performance in conversion and selectivity to methane. In addition, mesoporous structured materials with high porous volume and size also contribute to high catalytic activity. An optimum catalyst should have a high specific surface area and ultrafine or nanostructured particles of the metal active sites. It is important to characterize systematically the nature of the active sites and interactions among active components, support, and promoter to be able to tailor the structure of the catalyst. For practical CO_2 utilization, however, better understanding of reaction mechanisms at atomic/molecular level is necessary for the rational design of high performance catalysts.

Commercialization of CO_2 methanation

In view of commercialization of CO_2 methanation, this process is viable if the CO_2 and H_2 were generated from waste and renewable energy, respectively (Fig. 9). For instance, CO_2 can be generated from local biomass or power plants and H_2 can be produced *via* water electrolysis using inexpensive renewable power sources.

Renewable energy sources including wind, solar, hydro and geothermal as well nuclear energy that are bound to play an increasing role in the world's energy mix, produce primarily electricity. However, the current most promising renewable power source is hydroelectric power. Presently, hydroelectric power is by far the world's largest renewable source of electricity, with about 850 GW of installed capacity and an annual production of over 3 PWh.[100] In terms of electricity produced, it is second only to fossil fuel and generates about 10 times more power than geothermal, solar and wind power combined.[101] Hydroelectricity generation is based on turbines that convert the energy of falling water into mechanical power with an efficiency of about 90%.

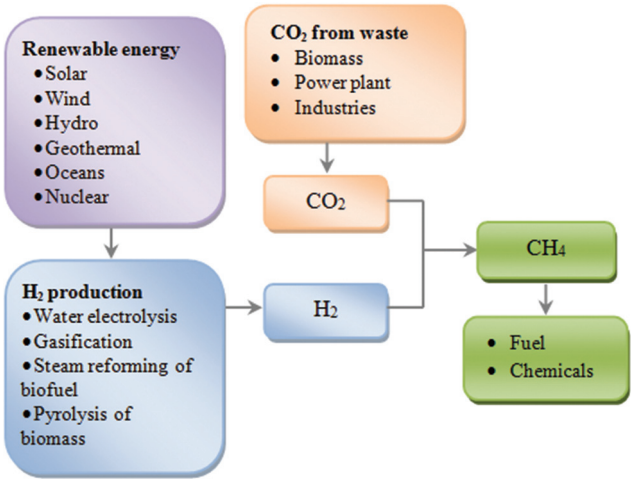

Fig. 9 Overview of CO_2 methanation.

In terms of the generation of hydrogen from renewable energy, the splitting of water would be the simplest way to produce synthetic hydrogen. The sole practical method to split water into hydrogen today is electrolysis, but others such as photochemical and thermal splitting as well as high temperature chemical cycles (*vide infra*) are also under investigation. Electrolysis of water has been practised for more than 100 years and is efficient with overall system conversions higher than 75 to 80%, with further improvements possible.

In general, water is concluded to be the only suitable source of hydrogen for reducing CO_2 emissions from various sources *via* its hydrogenation to methane. While having these advantages of availability, flexibility and high purity, to achieve widespread application hydrogen production using water electrolysis still needs improvements in energy efficiency, safety, durability, operability and portability and, above all, reduction in costs of installation and operation. These open up many new opportunities for research and development leading to technological advancements in water electrolysis.

Furthermore, the economy will be significantly improved when novel cost- and energy-efficient methods for providing large amounts of pure CO_2 are developed. Many industrial processes (Fig. 10), most notably power generation, cement manufacture, refineries and iron and steel making also intrinsically produce CO_2 and can be fitted with CO_2 capture

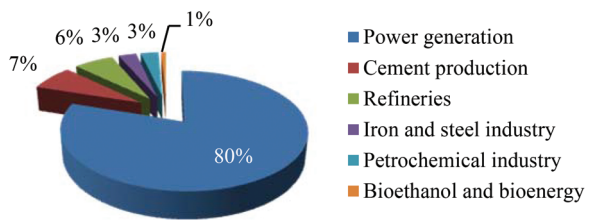

Fig. 10 Total annual CO_2 emissions in various industry sectors. Adopted from Metz *et al.*[102]

technologies. Currently, carbon capture and storage (CCS) offers one of the very few remaining methods to reduce CO_2 emissions. The captured CO_2 is then pressurized to 100 bar (or more), prior to being transported to a storage site and then later being used in a methanation unit. After all, as a green carbon source and renewable feedstock, the methanation of CO_2 definitely has a promising future.

Acknowledgements

This work was supported by the Ministry of Science, Technology and Innovation, Malaysia through EScienceFund Research grant no. 03-01-06-SF0987, MyPhd Scholarship (Muhammad Arif Ab Aziz) from Ministry of Higher Education, Malaysia.

Notes and references

1 P. Nema, S. Nema and P. Roy, *Renewable Sustainable Energy Rev.*, 2012, **16**, 2329.
2 G. A. Meehl, W. M. Washington, W. D. Collins, J. M. Arblaster, A. Hu, L. E. Buja, W. G. Strand and H. Teng, *Science*, 2005, **307**, 1769.
3 T. Sakakura, J.-C. Choi and H. Yasuda, *Chem. Rev.*, 2007, **107**, 2365.
4 R. L. Paddock and S. T. Nguyen, *J. Am. Chem. Soc.*, 2001, **123**, 11498.
5 D. Day, R. J. Evans, J. W. Lee and D. Reicosky, *Energy*, 2005, **30**, 2558.
6 K. A. Pokrovski and A. T. Bell, *J. Catal.*, 2006, **244**, 43.
7 W.-L. Dai, S.-L. Luo, S.-F. Yin and C.-T. Au, *Appl. Catal., A*, 2009, **366**, 2.
8 T. Iijima and T. Yamaguchi, *Appl. Catal., A*, 2008, **345**, 12.
9 H. Arakawa, M. Aresta, J. N. Armor, M. A. Barteau, E. J. Beckman, A. T. Bell, J. E. Bercaw, C. Creutz, E. Dinjus, D. A. Dixon, K. Domen, D. L. DuBois, J. Eckert, E. Fujita, D. H. Gibson, W. A. Goddard, D. W. Goodman, J. Keller, G. J. Kubas, H. H. Kung, J. E. Lyons, L. E. Manzer, T. J. Marks, K. Morokuma, K. M. Nicholas, R. Periana, L. Que, J. Rostrup-Nielson, W. M. H. Sachtler, L. D. Schmidt, A. Sen, G. A. Somorjai, P. C. Stair, B. R. Stults and W. Tumas, *Chem. Rev.*, 2001, **101**, 953.
10 Q. Zhang, Y.-Z. Zuo, M.-H. Han, J.-F. Wang, Y. Jin and F. Wei, *Catal. Today*, 2010, **150**, 55.
11 G. Bonura, M. Cordaro, C. Cannilla, F. Arena and F. Frusteri, *Appl. Catal., B*, 2014, **152–153**, 152.
12 A. Beuls, C. Swalus, M. Jacquemin, G. Heyen, A. Karelovic and P. Ruiz, *Appl. Catal., B*, 2012, **113–114**, 2.
13 T. Inui and T. Takeguchi, *Catal. Today*, 1991, **10**, 95.
14 A. D. Tomsett, T. Hagiwara, A. Miyamoto and T. Inui, *Appl. Catal.*, 1986, **26**, 391.
15 P. J. Lunde and F. L. Kester, *Ind. Eng. Chem. Process Des. Dev.*, 1974, **13**, 27.
16 K. R. Thampi, J. Kiwi and M. Gratzel, *Nature*, 1987, **327**, 506.
17 I. Alstrup, *J. Catal.*, 1995, **151**, 216.
18 C. Galletti, S. Specchia, G. Saracco and V. Specchia, *Chem. Eng. Sci.*, 2010, **65**, 590.
19 D. P. van der Wiel, J. L. Zilka-Marco, Y. Wang, A. Y. Tonkovich and R. S. Wegeng, *Carbon Dioxide Conversions in Microreactors*, American Institute of Chemical Engineers, 2000.
20 W. Wang and J. Gong, *Front. Chem. Sci. Eng.*, 2011, **5**, 2.
21 M. Cai, J. Wen, W. Chu, X. Cheng and Z. Li, *J. Nat. Gas Chem.*, 2011, **20**, 318.
22 S.-H. Kang, J.-H. Ryu, J.-H. Kim, S.-J. Seo, Y.-D. Yoo, P. Sai Prasad, H.-J. Lim and C.-D. Byun, *Korean J. Chem. Eng.*, 2011, **28**, 2282.
23 F. Ocampo, B. Louis, L. Kiwi-Minsker and A.-C. Roger, *Appl. Catal., A*, 2011, **392**, 36.
24 G. Zhi, X. Guo, Y. Wang, G. Jin and X. Guo, *Catal. Commun.*, 2011, **16**, 56.
25 D. C. D. da Silva, S. Letichevsky, L. E. P. Borges and L. G. Appel, *Int. J. Hydrogen Energy*, 2012, **37**, 8923.
26 S. Tada, T. Shimizu, H. Kameyama, T. Haneda and R. Kikuchi, *Int. J. Hydrogen Energy*, 2012, **37**, 5527.
27 C. Swalus, M. Jacquemin, C. Poleunis, P. Bertrand and P. Ruiz, *Appl. Catal., B*, 2012, **125**, 41.
28 R. Razzaq, H. Zhu, L. Jiang, U. Muhammad, C. Li and S. Zhang, *Ind. Eng. Chem. Res.*, 2013, **52**, 2247.
29 M. Gabrovska, R. Edreva-Kardjieva, D. Crişan, P. Tzvetkov, M. Shopska and I. Shtereva, *React. Kinet., Mech. Catal.*, 2012, **105**, 79.
30 H. Zhu, R. Razzaq, C. Li, Y. Muhmmad and S. Zhang, *AIChE J.*, 2013, **59**, 2567.
31 E. Jwa, S. B. Lee, H. W. Lee and Y. S. Mok, *Fuel Process. Technol.*, 2013, **108**, 89.
32 S. Hwang, U. Hong, J. Lee, J. Baik, D. Koh, H. Lim and I. Song, *Catal. Lett.*, 2012, **142**, 860.
33 P. A. U. Aldana, F. Ocampo, K. Kobl, B. Louis, F. Thibault-Starzyk, M. Daturi, P. Bazin, S. Thomas and A. C. Roger, *Catal. Today*, 2013, **215**, 201.
34 H. Liu, X. Zou, X. Wang, X. Lu and W. Ding, *J. Nat. Gas Chem.*, 2012, **21**, 703.
35 J. Liu, C. Li, F. Wang, S. He, H. Chen, Y. Zhao, M. Wei, D. G. Evans and X. Duan, *Catal. Sci. Technol.*, 2013, **3**, 2627.
36 B. Lu and K. Kawamoto, *Fuel*, 2013, **103**, 699.
37 A. Borgschulte, N. Gallandat, B. Probst, R. Suter, E. Callini, D. Ferri, Y. Arroyo, R. Erni, H. Geerlings and A. Zuttel, *Phys. Chem. Chem. Phys.*, 2013, **15**, 9620.
38 X. Zhang, W.-j. Sun and W. Chu, *J. Fuel Chem. Technol.*, 2013, **41**, 96.
39 S. He, C. Li, H. Chen, D. Su, B. Zhang, X. Cao, B. Wang, M. Wei, D. G. Evans and X. Duan, *Chem. Mater.*, 2013, **25**, 1040.
40 S. Hwang, J. Lee, U. G. Hong, J. H. Baik, D. J. Koh, H. Lim and I. K. Song, *J. Ind. Eng. Chem.*, 2013, **19**, 698.
41 M. A. A. Aziz, A. A. Jalil, S. Triwahyono, R. R. Mukti, Y. H. Taufiq-Yap and M. R. Sazegar, *Appl. Catal., B*, 2014, **147**, 359.

42 M. A. A. Aziz, A. A. Jalil, S. Triwahyono and S. M. Sidik, *Appl. Catal., A*, 2014, **486**, 115.
43 M. A. A. Aziz, A. A. Jalil, S. Triwahyono and M. W. A. Saad, *Chem. Eng. J.*, 2015, **260**, 757.
44 W. Cai, Q. Zhong and Y. Zhao, *Catal. Commun.*, 2013, **39**, 30.
45 W. A. Wan Abu Bakar, R. Ali, A. A. A. Kadir, S. J. M. Rosid and N. S. Mohammad, *J. Fuel Chem. Technol.*, 2012, **40**, 822.
46 P. Bothra, G. Periyasamy and S. K. Pati, *Phys. Chem. Chem. Phys.*, 2013, **15**, 5701.
47 Q. Pan, J. Peng, S. Wang and S. Wang, *Catal. Sci. Technol.*, 2014, **4**, 502.
48 I. Graça, L. V. González, M. C. Bacariza, A. Fernandes, C. Henriques, J. M. Lopes and M. F. Ribeiro, *Appl. Catal., B*, 2014, **147**, 101.
49 S. Rahmani, M. Rezaei and F. Meshkani, *J. Ind. Eng. Chem.*, 2014, **20**, 1346.
50 S. Kato, A. Borgschulte, D. Ferri, M. Bielmann, J.-C. Crivello, D. Wiedenmann, M. Parlinska-Wojtan, P. Rossbach, Y. Lu, A. Remhof and A. Zuttel, *Phys. Chem. Chem. Phys.*, 2012, **14**, 5518.
51 S. Abelló, C. Berrueco and D. Montané, *Fuel*, 2013, **113**, 598.
52 G. Garbarino, P. Riani, L. Magistri and G. Busca, *Int. J. Hydrogen Energy*, 2014, **39**, 11557.
53 P. Riani, G. Garbarino, M. A. Lucchini, F. Canepa and G. Busca, *J. Mol. Catal. A: Chem.*, 2014, **383–384**, 10.
54 M. Guo and G. Lu, *Catal. Commun.*, 2014, **54**, 55.
55 W. Zhen, B. Li, G. Lu and J. Ma, *Chem. Commun.*, 2015, **51**, 1728.
56 X. Lu, F. Gu, Q. Liu, J. Gao, Y. Liu, H. Li, L. Jia, G. Xu, Z. Zhong and F. Su, *Fuel Process. Technol.*, 2014, DOI: 10.1016/j.fuproc.2014.10.009.
57 H. Lu, X. Yang, G. Gao, K. Wang, Q. Shi, J. Wang, C. Han, J. Liu, M. Tong, X. Liang and C. Li, *Int. J. Hydrogen Energy*, 2014, **39**, 18894.
58 M. Guo and G. Lu, *RSC Adv.*, 2014, **4**, 58171.
59 C. K. Vance and C. H. Bartholomew, *Appl. Catal.*, 1983, **7**, 169.
60 T. Mitsui, M. K. Rose, E. Fomin, D. F. Ogletree and M. Salmeron, *Nature*, 2003, **422**, 705.
61 Z. Yan, S. Chinta, A. A. Mohamed, J. P. Fackler and D. W. Goodman, *J. Am. Chem. Soc.*, 2005, **127**, 1604.
62 V. Ortalan, A. Uzun, B. C. Gates and N. D. Browning, *Nat. Nanotechnol.*, 2010, **5**, 843.
63 H. Hattori, *Appl. Catal., A*, 2001, **222**, 247.
64 T. Mori, H. Masuda, H. Imai, A. Miyamoto, S. Baba and Y. Murakami, *J. Phys. Chem.*, 1982, **86**, 2753.
65 H. Schaper, E. B. M. Doesburg, P. H. M. De Korte and L. L. Van Reijen, *Appl. Catal.*, 1985, **14**, 371.
66 K. O. Xavier, R. Sreekala, K. K. A. Rashid, K. K. M. Yusuff and B. Sen, *Catal. Today*, 1999, **49**, 17.
67 P. Djinović, C. Galletti, S. Specchia and V. Specchia, *Top. Catal.*, 2011, **54**, 1042.
68 S. Sharma, Z. Hu, P. Zhang, E. W. McFarland and H. Metiu, *J. Catal.*, 2011, **278**, 297.
69 D. Theleritis, S. Souentie, A. Siokou, A. Katsaounis and C. G. Vayenas, *ACS Catal.*, 2012, **2**, 770.
70 P. Panagiotopoulou, D. I. Kondarides and X. E. Verykios, *Catal. Today*, 2012, **181**, 138.
71 Y. Zhu, S. Zhang, Y. Ye, X. Zhang, L. Wang, W. Zhu, F. Cheng and F. Tao, *ACS Catal.*, 2012, **2**, 2403.
72 J. H. Kwak, L. Kovarik and J. Szanyi, *ACS Catal.*, 2013, **3**, 2094.
73 S. Eckle, M. Augustin, H.-G. Anfang and R. J. Behm, *Catal. Today*, 2012, **181**, 40.
74 S. Akamaru, T. Shimazaki, M. Kubo and T. Abe, *Appl. Catal., A*, 2014, **470**, 405.
75 D. C. Upham, A. R. Derk, S. Sharma, H. Metiu and E. W. McFarland, *Catal. Sci. Technol.*, 2015, **5**, 1783.
76 A. L. Kustov, A. M. Frey, K. E. Larsen, T. Johannessen, J. K. Nørskov and C. H. Christensen, *Appl. Catal., A*, 2007, **320**, 98.
77 M. Agnelli, M. Kolb and C. Mirodatos, *J. Catal.*, 1994, **148**, 9.
78 M. Agnelli, H. M. Swaan, C. Marquez-Alvarez, G. A. Martin and C. Mirodatos, *J. Catal.*, 1998, **175**, 117.
79 A. Karelovic and P. Ruiz, *Appl. Catal., B*, 2012, **113–114**, 237.
80 A. Karelovic and P. Ruiz, *J. Catal.*, 2013, **301**, 141.
81 M. Tóth, J. Kiss, A. Oszkó, G. Pótári, B. László and A. Erdőhelyi, *Top. Catal.*, 2012, **55**, 747.
82 A. Karelovic and P. Ruiz, *ACS Catal.*, 2013, **3**, 2799.
83 S. K. Beaumont, S. Alayoglu, C. Specht, W. D. Michalak, V. V. Pushkarev, J. Guo, N. Kruse and G. A. Somorjai, *J. Am. Chem. Soc.*, 2014, **136**, 9898.
84 J. Martins, N. Batail, S. Silva, S. Rafik-Clement, A. Karelovic, D. P. Debecker, A. Chaumonnot and D. Uzio, *Catal. Commun.*, 2015, **58**, 11.
85 N. Srisawad, W. Chaitree, O. Mekasuwandumrong, A. Shotipruk, B. Jongsomjit and J. Panpranot, *React. Kinet., Mech. Catal.*, 2012, **107**, 179.
86 G. Zhou, T. Wu, H. Xie and X. Zheng, *Int. J. Hydrogen Energy*, 2013, **38**, 10012.
87 R. Razzaq, C. Li, M. Usman, K. Suzuki and S. Zhang, *Chem. Eng. J.*, 2015, **262**, 1090.
88 V. Iablokov, S. K. Beaumont, S. Alayoglu, V. V. Pushkarev, C. Specht, J. Gao, A. P. Alivisatos, N. Kruse and G. A. Somorjai, *Nano Lett.*, 2012, **12**, 3091.
89 J. Janlamool, P. Praserthdam and B. Jongsomjit, *J. Nat. Gas Chem.*, 2011, **20**, 558.
90 M. A. Vannice, *J. Catal.*, 1976, **44**, 152.
91 J. Krause, D. Borgmann and G. Wedler, *Surf. Sci.*, 1996, **347**, 1.
92 C. F. Zinola, C. Gomis-Bas, G. L. Estiú, E. A. Castro and A. J. Arvia, *Langmuir*, 1998, **14**, 3901.
93 A. Berkó and F. Solymosi, *Vacuum*, 1987, **37**, 196.
94 S.-G. Wang, X.-Y. Liao, D.-B. Cao, C.-F. Huo, Y.-W. Li, J. Wang and H. Jiao, *J. Phys. Chem. C*, 2007, **111**, 16934.
95 X. Ding, V. Pagan, M. Peressi and F. Ancilotto, *Mater. Sci. Eng., C*, 2007, **27**, 1355.

96 K. R. Hahn, M. Iannuzzi, A. P. Seitsonen and J. Hutter, *J. Phys. Chem. C*, 2013, **117**, 1701.
97 S.-i. Fujita, M. Nakamura, T. Doi and N. Takezawa, *Appl. Catal., A*, 1993, **104**, 87.
98 J. J. Benítez, R. Alvero, M. J. Capitán, I. Carrizosa and J. A. Odriozola, *Appl. Catal.*, 1991, **71**, 219.
99 R. A. D. Betta and M. Shelef, *J. Catal.*, 1977, **48**, 111.
100 World Energy Council, *2010 Survey of Energy Resources*, http://www.worldenergy.org/.
101 Q. Schiermeier, J. Tollefson, T. Scully, A. Witze and O. Morton, *Nature*, 2008, **454**, 816.
102 B. Metz, O. Davidson, H. de Coninck, M. Loos and L. Meyer, *Carbon Dioxide Capture Storage*, 2005.